0026-895X/01/6005-907–915$3.00
MOLECULAR PHARMACOLOGY
Vol. 60, No. 5
891/936155
Mol Pharmacol 60:907–915, 2001
Printed in U.S.A.

Enhanced Acetaminophen Hepatotoxicity in Transgenic Mice Overexpressing BCL-2

MICHAEL L. ADAMS, ROBERT H. PIERCE, MARY E. VAIL, COLLIN C. WHITE, ROBERT P. TONGE,[1] TERRENCE J. KAVANAGH, NELSON FAUSTO, SIDNEY D. NELSON, and SAM A. BRUSCHI

Departments of Medicinal Chemistry (M.L.A., R.P.T., S.D.N., S.A.B.), Environmental Health (C.C.W., T.J.K.), Pathology (N.F.), and Molecular and Cellular Biology Program (M.E.V.), University of Washington, Seattle, Washington; and Department of Pathology and Laboratory Medicine (R.H.P.), University of Rochester School of Medicine and Dentistry, Rochester, New York

Received February 15, 2001; accepted July 19, 2001

This paper is available online at http://molpharm.aspetjournals.org

ABSTRACT

Mitochondria play an important role in the cell death induced by many drugs, including hepatotoxicity from overdose of the popular analgesic, acetaminophen (APAP). To investigate mitochondrial alterations associated with APAP-induced hepatotoxicity, the subcellular distribution of proapoptotic BAX was determined. Based on the antiapoptotic characteristics of BCL-2, we further hypothesized that if a BAX component was evident then BCL-2 overexpression may be hepatoprotective. Mice, either with a human *bcl-2* transgene (−/+) or wild-type mice (WT; −/−), were dosed with 500 or 600 mg/kg (i.p.) APAP or a nonhepatotoxic isomer, *N*-acetyl-*m*-aminophenol (AMAP). Immunoblot analyses indicated increased mitochondrial BAX-β content very early after APAP or AMAP treatment. This was paralleled by disappearance of BAX-α from the cytosol of APAP treated animals and, to a lesser extent, with AMAP treatment. Early pathological evidence of APAP-induced zone 3 necrosis was seen in *bcl-2* (−/+) mice, which progressed to massive panlobular necrosis with hemorrhage by 24 h. In contrast, WT mice dosed with APAP showed a more typical, and less severe, centrilobular necrosis. AMAP-treated *bcl-2* (−/+) mice displayed only early microvesicular steatosis without progression to extensive necrosis. Decreased complex III activity, evident as early as 6 h after treatment, correlated well with plasma enzyme activities at 24 h (AST $r^2 = 0.89$, ALT $r^2 = 0.87$) thereby confirming a role for mitochondria in APAP-mediated hepatotoxicity. In conclusion, these data suggest for the first time that BAX may be an early determinant of APAP-mediated hepatotoxicity and that BCL-2 overexpression unexpectedly enhances APAP hepatotoxicity.

An important role for mitochondria is frequently observed during apoptosis or drug-induced cell death. Although the exact contribution of this organelle in APAP-induced liver injury and cell death is unclear, alterations to mitochondrial respiration with APAP treatments have been demonstrated (Burcham and Harman, 1991). Mechanistically, the arylation of free thiols (Qiu et al., 1998b) as well as oxidative stress (Adamson and Harman, 1993) have been proposed to play roles in the toxicity of APAP, but the consequences of these changes are still uncertain (Pumford and Halmes, 1997). More recent studies have identified proteins covalently modified by APAP or its less hepatotoxic isomer *N*-acetyl-*m*-aminophenol (AMAP), and indicate that an important component of the differential toxicity of these compounds is mediated at the level of the mitochondrion (Qiu et al., 1998a,b).

The hepatotoxicity of APAP has been traditionally thought of as a centrilobular necrotic event (Pumford and Halmes, 1997). Other studies have attempted to define an apoptotic component to APAP-mediated cell death, but these investigations have not been entirely definitive (Ray et al., 1996; Lawson et al., 1999). Consequently, we have addressed the possibility that the BCL-2 family of proteins may have a functional role in the progression of liver damage after APAP overdose. The BCL-2 protein family consists of both proapoptotic (e.g., BAX, BAK) and antiapoptotic (e.g., BCL-2, BCL-X_L) members, which play an important role in the determination of apoptosis in response to many physiological and pathological effectors (Wei et al., 2001). This pro- versus

This work was supported by National Institutes of Health Grants GM51916 (S.B.), GM25418 (S.D.N.), CA74131 (N.F.), and ES04696 (T.J.K.), National Institute of Environmental Health Sciences Center Grant P30-ES07033, National Institutes of Health Training Grant GM07750 (M.L.A.), and United States Public Health Service National Research Grant T32-GM07270 (M.E.V.).

[1] Current address: Zeneca Pharmaceuticals, Alderly Park, Macclesfield, Cheshire, England, UK

ABBREVIATIONS: APAP, *N*-acetyl-*p*-aminophenol; AMAP, *N*-acetyl-*m*-aminophenol; *bcl-2,* gene/coding sequence for human BCL-2 protein; ALT, alanine aminotransferase; AST, aspartate aminotransferase; GSH, reduced glutathione; GSSG, oxidized glutathione; HPLC, high-performance liquid chromatography; Ac-DEVD-amc, acetyl-Asp-Glu-Val-Asp-aminomethylcoumarin; WT, wild-type; NAPQI, *N*-acetyl-*p*-benzoquinone imine; GAPDH, glyceraldehyde-3-phosphate dehydrogenase.

antiapoptotic balance has been suggested to be controlled through dimerization of BCL-2 family members (Yin et al., 1994; Rosse et al., 1998) and/or by phosphorylation (Haldar et al., 1998). Although there is an extensive literature on the antiapoptotic properties of BCL-2, its mechanism of cytoprotection is still unknown. It has been proposed that the cytoprotective action of BCL-2 may lie in its ability to act as an antioxidant (Hockenbery et al., 1993), to block cytochrome *c* release (Cai and Jones, 1998), or to inhibit caspase activity after cytochrome *c* release (Rosse et al., 1998). Further studies are consequently required to address this uncertainty in BCL-2 function, particularly with recent reports indicating that BAX translocation to mitochondria is not prevented in apoptotic neurons despite overexpression of BCL-2 (Putcha et al., 1999).

Based on observations that APAP-induced cell death is partly apoptotic (Ray et al., 1996; Lawson et al., 1999), we examined APAP-mediated hepatotoxicity for alterations to the subcellular distribution of BAX, a BCL-2 family member implicated as a central effector of mitochondrially-mediated apoptotic cell death (Wei et al., 2001). We report here that BAX is redistributed with APAP treatment and, consequently, may play an early role in APAP-mediated hepatotoxicity. In addition, we hypothesized that overexpression of BCL-2 protein should offer protection to liver tissue exposed to doses of APAP that would otherwise cause centrilobular necrosis. Our results indicate a more pronounced liver injury produced by APAP in BCL-2–overexpressing animals with morphological and biochemical evidence of increased damage shifting from centrilobular to throughout the entire lobule (panlobular). These unexpected findings provide a basis for the further elucidation of the role of mitochondria in APAP-induced liver injury and cell death.

Materials and Methods

Animal Care and Dosing Protocols. Human *bcl-2* transgenic mice (C57/B6C3H background) were kindly provided by Dr. S. J. Korsmeyer (Dana-Farber Cancer Institute, Harvard Medical School, Boston, MA). Animals were housed in a temperature- and humidity-controlled specific pathogen free facility maintained on a 12-h light/dark cycle with free access to food and water. Animals were genotyped using tail DNA in a polymerase chain reaction assay. Briefly, tail snips were digested in proteinase K overnight at 55°C. Proteinase K was then heat inactivated at 95°C for 10 min. Polymerase chain reaction was performed using 1 μl of the crude extract as a template and primers spanning an intron in *bcl-2* to yield a 300-base-pair product from the human gene. BCL-2 expression is under the inducible control of a metallothionein promoter. Male mice 16 weeks old (22–28 g) were given 25 mM $ZnSO_4$ in drinking water for 5 to 7 days prior to dosing and BCL-2 levels were evaluated by immunoblot. Animals were fasted for 16 h before dosing with APAP or AMAP (500 mg/kg i.p.) or vehicle (saline). To exclude nonspecific metal effects, $ZnSO_4$-supplemented water was freely available to all animals during the fast and after dosing. Liver tissue and plasma samples were taken 6 and 24 h after injection for histopathological, immunoblotting, and other biochemical determinations.

Isolation of Subcellular Fractions and Immunoblotting Procedures. BAX subcellular localization studies were with fractions prepared by standard differential centrifugation procedures from wild-type $B6C3F_1$ (Fig. 1) or Swiss-Webster mice (data not presented) receiving 600 mg/kg (i.p.) APAP, AMAP, or vehicle control (saline) at 2 and/or 4 h after dosing as described previously (Tonge et al., 1998). The relative purity of subcellular fractions was assessed by monitoring lactate dehydrogenase (cytosol) and succinate cytochrome *c* reductase (mitochondria) marker enzyme activities. Subcellular fractions or total homogenized liver tissue (50 μg per lane) were resolved on SDS-polyacrylamide minigels (10 to 15%, Mini-Protean II; Bio-Rad, Hercules, CA) and transferred to nitrocellulose (1 h, 15 V, Trans-Blot SD SemiDry Transfer Cell; BioRad). Immunodetection using antibodies to BAX (B9; Santa Cruz Biotechnology, Santa Cruz, CA), BCL-2 (N19; Santa Cruz Biotechnology), catalase (Calbiochem, San Diego, CA), cytochrome *c* (Pharmingen, San Diego, CA), mouse albumin (ICN Pharmaceuticals, Costa Mesa, CA), GAPDH (Dietze et al., 1997), or anti-APAP protein adducts (Tonge et al., 1998) was preformed by standard procedures and detected by chemiluminescence (SuperSignal ULTRA; Pierce, Rockford, IL).

Transaminase Activities. Alanine aminotransferase (ALT) and aspartate aminotransferase (AST) were assessed spectrophotometrically using either the *Dimension Clinical Chemistry System* (Dade Behring, Deerfield, IL) analyzer on plasma samples diluted with DADE diluent to within the linear range of the analyzer (typically 1:40–1:50) or standard commercial methods (Sigma Diagnostics Infinity, Procedure 122-UV or 152-UV) exactly as described by the manufacturer. In both cases aminotransferase activities are presented as units per liter.

Assessment of Hepatotoxicity by Histopathology. Liver tissue sections from animals dosed with APAP, AMAP, or saline were fixed in formalin and embedded in paraffin. Sections of 5-μm thickness were stained with hematoxylin and eosin using standard procedures. Sections were independently evaluated without prior knowledge of treatment regime and digital photomicrographs were taken at 100× or 200× magnification.

Assessment of Cellular Morphology by Electron Microscopy. Liver sections from animals dosed with APAP, AMAP, or saline were fixed in Karnovsky's fixative (one-half strength glutaraldehyde-formaldehyde), embedded and stained with uranyl acetate and Reynold's lead citrate. Specimens were examined using a Philips

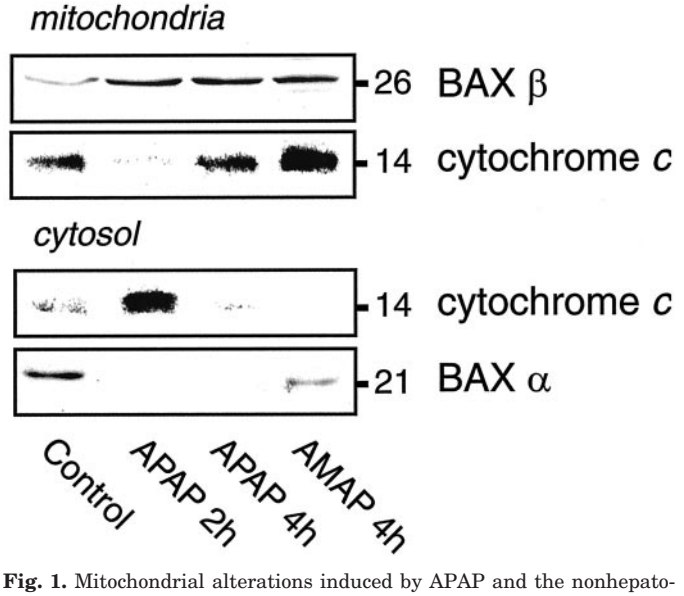

Fig. 1. Mitochondrial alterations induced by APAP and the nonhepatotoxic positional isomer, AMAP. Subcellular fractions from $B6C3F_1$ mice were isolated at various times after control (vehicle), APAP, or AMAP treatment (600 mg/kg, i.p) and immunoblotted using standard procedures. Top two blots, mitochondrial fractions immunoblotted for BAX and cytochrome *c* content indicated early and sustained BAX-β relocalization to mitochondria in all treatments with transient cytochrome *c* depletion in APAP treatments. Bottom two blots, cytosolic fractions immunoblotted for BAX and cytochrome *c* release indicated release of cytochrome *c* from mitochondria of APAP-treated animals and either an absence of BAX-α immunoreactivity in APAP treatments or a relative depletion of BAX-α in AMAP-treated animals. Molecular mass of immunoreactive proteins, in kilodaltons, is indicated on the right of each blot.

410 Transmission Electron Microscope at 12,000× or 6,000× magnification.

Determination of Reduced (GSH) and Oxidized (GSSG) Liver Glutathione Content. Hepatic glutathione levels were determined as described previously (Luderer et al., 2001). Briefly, liver tissue was homogenized in 5% (w/v) sulfosalicylic acid then immediately processed independently for either GSH or GSSG. For GSSG, free GSH was derivatized with 2-vinylpyridine at room temperature and excess 2-vinylpyridine extracted into the organic phase with chloroform. GSSG was then reduced by the addition of 50 μl of 1 mM NADPH and 20 units/ml GSH reductase for 1 h at room temperature, followed by derivatization with 20 μl of 12.5 mM monobromobimane in the dark for 30 min before HPLC analysis (Shimadzu LC-6A HPLC equipped with an Alltech 15 × 0.5-cm C18 reversed-phase column using a binary gradient [solvent A, 1.0 mM tetrabutylammonium phosphate, pH 3.0; solvent B, methanol] at a flow rate of 1.5 ml/min with starting conditions of 95% A/5% B). Eluted peaks were monitored fluorometrically at λex = 375 nm and λem = 475 nm. Reduced GSH was assessed by further dilution (1:10) with 5% (w/v) sulfosalicylic acid. A 100-μl volume of the diluted sample was then combined with 50 μl 10% (v/v) triethanolamine, mixed, and 100 μl of the mixture was added to 200 μl of buffer (100 mM NaH_2PO_4, 1 mM EDTA) before derivatization and HPLC as described above for GSSG.

Caspase Activation. Caspase activation was determined as described previously (Franklin et al., 1998). Briefly, 50 μg of liver tissue homogenate were incubated for 60 min at 37°C in 100 μl of caspase assay buffer [50 mM HEPES, pH 7.4, 100 mM sodium chloride, 2 mM EDTA, 20% sucrose (w/v), 0.2% CHAPS (w/v), 10 mM DTT] with 20 μM Ac-DEVD-amc (Alexis Biochemicals, San Diego, CA) and fluorescence monitored on a Packard Fluorocount (Packard Instrument Company, Meriden, CT) microplate fluorometer with an excitation wavelength of 360 nm and an emission wavelength of 460 nm. Data are presented as fold activation over extracts from untreated cells.

Determination of Mitochondrial Respiration. Oxidative phosphorylation activity, via complex III, ubiquinol:ferricytochrome *c* oxidoreductase (E. C. 1.10.2.2), was assayed as described previously (Gudz et al., 1997). In brief, the rate of reduction of cytochrome *c* in isolated mitochondria was monitored spectrophotometrically (Cary 3E UV-Vis Spectrophotometer, Varian, Australia) with or without antimycin A, a specific complex III inhibitor, for 1 min at 550 nm after the addition of decylubiquinol substrate. The antimycin A sensitive rate is then calculated using the extinction coefficient of 19.1 mM^{-1} cm^{-1} (Gudz et al., 1997) and reported as micromoles of cytochrome *c* reduced per minute per milligram of mitochondrial protein.

Statistical Analysis. Results are calculated as mean ± S.E. Statistical significance was determined for transaminase and caspase activities using two-tailed, unpaired *t* test analysis and for GSH/GSSG contents using a paired, two-tailed *t* test. The statistical significance of complex III activities was determined by Mann-Whitney *U* test. Values for $p \leq 0.05$ were considered significant.

Results

Altered Processing and Subcellular Levels of BAX after Drug Treatment. Increased immunoreactivity of proapoptotic BAX was found in the mitochondrial fraction after APAP or AMAP treatment of wild-type $B6C3F_1$ mice (Fig. 1, top). Molecular mass calculations performed on the data indicated that in these nontransgenic animals, the β splice variant of BAX represented the active isoform. Similarly, a loss of BAX immunoreactivity from the cytosol, consistent with the BAX-α isoform, was observed (Fig. 1, bottom). Moreover, at these early time points the extent of BAX-α loss seemed to correlate well with the relative hepatotoxic potential of the two compounds being completely absent in the cytosol of APAP treatments only. Drug-induced increases to BAX-β mitochondrial levels, however, were associated only with release of cytochrome *c* into the cytosol in animals treated with APAP for 2 h and not observed with AMAP treatment (Fig. 1).

Assessment of Liver Damage. Liver damage was assessed histologically and by determining plasma ALT and AST activities. WT (−/−) and *bcl-2* (−/+) transgenic animals induced with zinc demonstrated no alterations to hepatic morphologies (compare Fig. 2, C and D, with Fig. 2A) and no significant differences in plasma ALT and AST levels (data not shown). Consequently, WT (−/−) animals were used as the basis for comparison with treatment groups. At 6 h after injection, all treatment transaminase levels were elevated compared with vehicle-treated control animals (Table 1). The 24-h ALT and AST enzyme levels were significantly raised in APAP-treated *bcl-2* (−/+) transgenic mice (55.8- and 18-fold higher, respectively) versus control (vehicle-treated) WT mice. In comparison, APAP-treatment in WT mice resulted in considerably smaller elevations of plasma ALT and AST activities versus control (vehicle-treated) WT mice (22- and 6.6-fold, respectively; Table 1). These 24-h data indicate a previously unreported difference in the biological response to APAP between WT and *bcl*-2 (−/+) animals with a more severe form of liver damage found in BCL-2 overexpressing mice.

In contrast to APAP treatment, AMAP-treated transgenic animals showed only early elevations in liver enzymes (6 h), which returned to uninjured (control) levels within 24 h, indicating a lack of progression to fulminant hepatotoxicity

TABLE 1

Plasma Transaminase Activities in wild-type (−/−) and *bcl-2* (−/+) transgenic mice treated with 500 mg/kg APAP or AMAP

Values are reported as Units per liter. [mean (S.E.)]. n = 3 to 6 for each treatment group.

	AST				ALT			
	6 h	F.C.	24 h	F.C.	6 h	F.C.	24 h	F.C.
Control (−/−)[a]	531 (361)		1,175 (446)		211 (31)		626 (262)	
APAP (−/−)	5,745 (1,004)[b]	10.8	7,787 (2380)[b,c]	6.6	6,258 (1,587)	29.7	13,746 (3,374)[b,c]	22.0
APAP (−/+)	3,764 (1,123)[b]	7.1	21,196 (882)[d,e,f]	18.0	3,278 (1,006)[b]	15.5	34,920 (5,604)[b,e,f]	55.8
AMAP (−/+)	1,010 (178)	1.9	564 (141)	0.5	725 (222)	3.4	543 (126)	0.9

F.C., Fold Change as compared with control values.
[a] No significant differences were observed between bcl-2 (−/−) and (−/+) in either plasma AST or ALT levels.
[b] $p \leq 0.05$ versus control (−/−).
[c] Dosed 6 animals, 3 survived.
[d] $p \leq 0.001$ versus control (−/−).
[e] Dosed 7 animals, 3 survived.
[f] $p \leq 0.05$ versus APAP (−/−) 24 h.

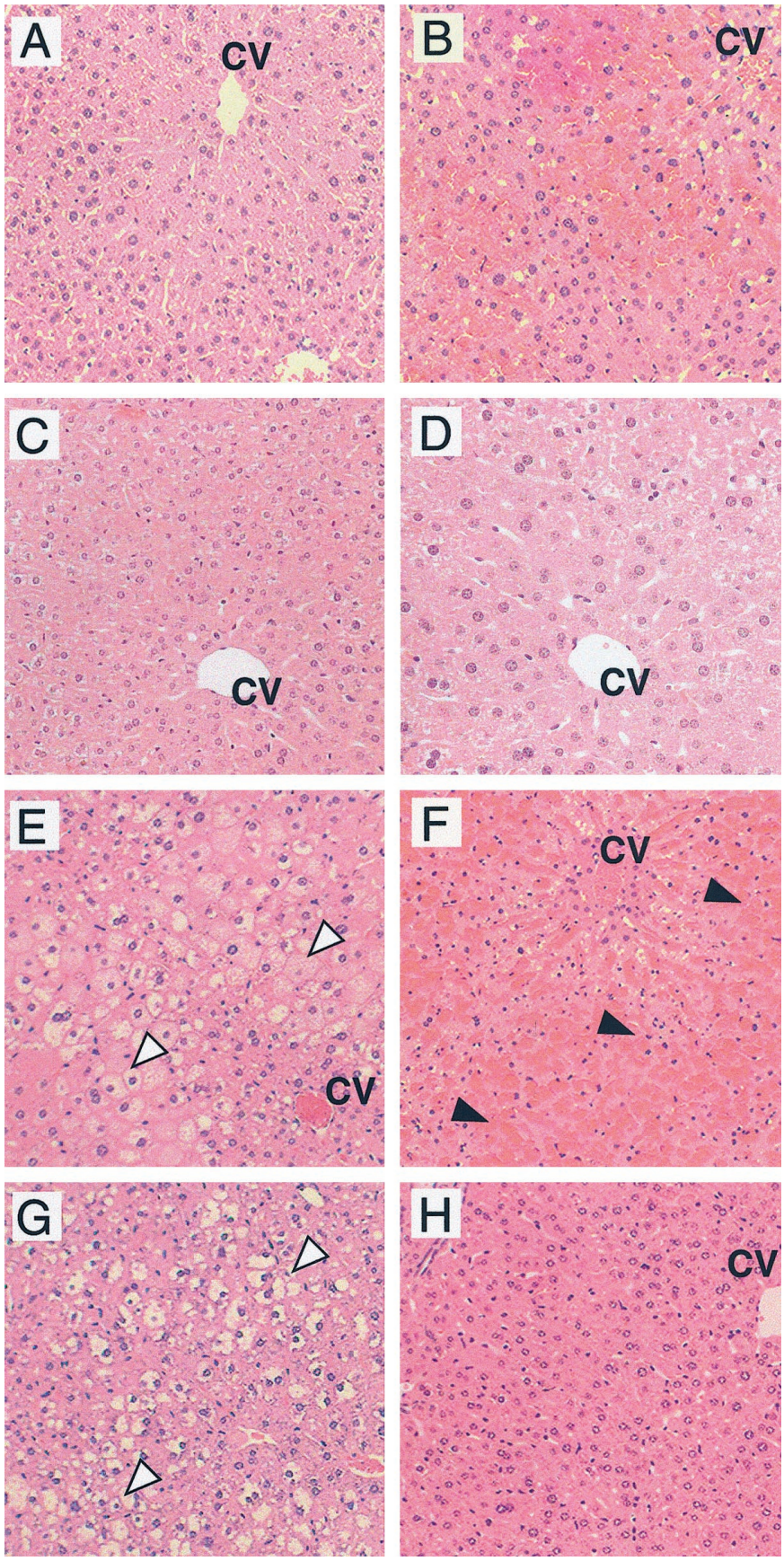

Fig. 2. Assessment of hepatotoxicity by morphology. Hematoxylin- and eosin-stained liver sections 6 and 24 h after dosing with APAP or AMAP (500 mg/kg, i.p.). All animals were induced with 25 mM $ZnSO_4$ in the drinking water for 5 to 7 days before dosing. A, control WT (−/−) treated with saline showing only normal hepatic morphology. B, WT (−/−) animals 24 h after dosing with APAP showing distinct areas of centrilobular necrosis. C–D, zinc-induced *bcl-2* (−/+) animals dosed with saline only at either 100× (C) or 200× (D) magnification showing typical hepatic lobule structure and no evidence of damage. E–F, *bcl-2* (−/+) animals 6 h (E) and 24 h (F) after dosing with APAP. At 6 h, microvesicular steatosis (hollow arrowheads, E) is observed, but by 24 h, a massive confluent necrosis is evident (solid arrowheads, F) with considerable hemorrhage. G–H, AMAP-treated animals developed a qualitatively more pronounced microvesicular steatosis at 6 h (hollow arrowheads, G). In contrast to APAP, AMAP-treated *bcl-2* (−/+) animals did not progress to extensive damage (H). All photographs are 100× magnification, except D is 200×. CV, central vein.

with this nonhepatotoxic isomer (Table 1). To exclude the possibility of increased metabolism and bioactivation of APAP in *bcl-2* (−/+) animals, we confirmed the extent of protein adduct formation at 6 and 24 h by immunoblot as described previously (Tonge et al., 1998). These data indicate that alterations to APAP-induced hepatotoxicity in BCL-2 overexpressing animals are not a result of increased production of the APAP reactive metabolite, NAPQI, because no difference in the extent of protein modification was detected (data not presented).

Histopathological Analyses. In comparison with vehicle-treated control animals (Fig. 2A), APAP treatment in WT mice resulted in a clear centrilobular (zone 3) necrosis with areas of focal bridging necrosis and hemorrhage (Fig. 2B). In places where the hepatocytes were less obscured by blood (i.e., at the edges of the lesion), microvesicular steatosis was also identified in intact centrilobular hepatocytes (data not shown).

Evidence of zone 3 necrosis and microvesicular steatosis was also observed after 6 h in *bcl-2* (−/+) transgenic mice treated with APAP (Fig. 2E). The pronounced microvesicular steatosis found at this time point was suggestive of an early injury marker presumably involving the endoplasmic reticulum and mitochondria (Redlich et al., 1990). In contrast to the more typical centrilobular injury of WT animals (Fig. 2B), APAP-induced damage in *bcl-2* (−/+) mice progressed to massive confluent necrosis and hemorrhagic infiltration by 24 h (Fig. 2F). Consequently, the extent of lobular involvement was much greater in BCL-2–overexpressing animals, indicating that BCL-2 overexpression was not hepatoprotective but instead exacerbated APAP-initiated liver damage.

BCL-2 overexpressing animals dosed with AMAP also developed microvesicular steatosis 6 h after treatment but did not progress to extensive necrosis (Fig. 2, G and H). Based on the extent of histopathologic changes, we conclude that AMAP is significantly less hepatotoxic compared with APAP in *bcl-2* (−/+) transgenic mice in keeping with previous reports using other mouse strains (Tirmenstein and Nelson, 1991).

BCL-2 overexpression per se had little effect on overall cellular morphology as observed by electron microscopy except for the presence of electron dense cytoplasmic aggregates in all *bcl-2* (−/+) mice induced with $ZnSO_4$ supplemented water (Fig. 3, A, C and D). Treatment of WT mice with APAP resulted in nuclear condensation and margination as well as mitochondrial proliferation (Fig. 3B). Increased lipid deposits were also apparent at 6 h after treatment with APAP consistent with the hepatic steatosis observed by light microscopy (Fig. 3B). Liver tissue morphology of BCL-2–overexpressing mice treated with APAP was distinctive, however, with mitochondrial/endoplasmic reticulum associations commonly observed (Fig. 3C). In addition, ringed mitochondria, which are often associated with hepatotoxicity in the rat (Ghadially, 1997), were observed (Fig. 3C). The functional significance of these structures are unknown but may be related to autophagy of this organelle (Dunn, 1990).

Further Characterizations of BCL-2 Overexpression in Control and APAP-Treated Animals. To further assess the effects of BCL-2 overexpression per se, several biochemical parameters were determined in addition to liver morphology. Early, APAP-specific increases in mitochondrial BAX content (and most likely BAX-α) were reproducibly observed in *bcl-2* (−/+) transgenic mice by chemiluminescent immunoblot analysis but required extended, overnight, exposures to be detected (Fig. 4A, top blot). In comparison, no differences in saline-treated mitochondrial BAX content were observed between *bcl-2* (−/−) and *bcl-2* (−/+) animals (Fig. 4A, top blot). However, APAP-specific BAX mitochondrial translocations in *bcl-2* (−/+) mice failed to induce cytochrome *c* release into the cytosol (Fig. 4A, middle blot) despite apparently excellent subcellular fractionations of mitochondria from the cytosol (cytochrome *c* versus GAPDH; Fig. 4A, middle and bottom blots).

Overexpression of BCL-2 was observed to marginally but significantly increase hepatic GSSG levels ($p < 0.05$) without significant alterations to reduced GSH (Fig. 4B). These data suggest that BCL-2 expression alone, without APAP treatment, may result in a basal oxidative stress, which does not manifest as overt injury by either morphological criteria or plasma transaminase elevations (Figs. 2 & 3, Table 1, *Discussion*). Furthermore, although alterations were not observed in total cellular catalase or copper/zinc superoxide

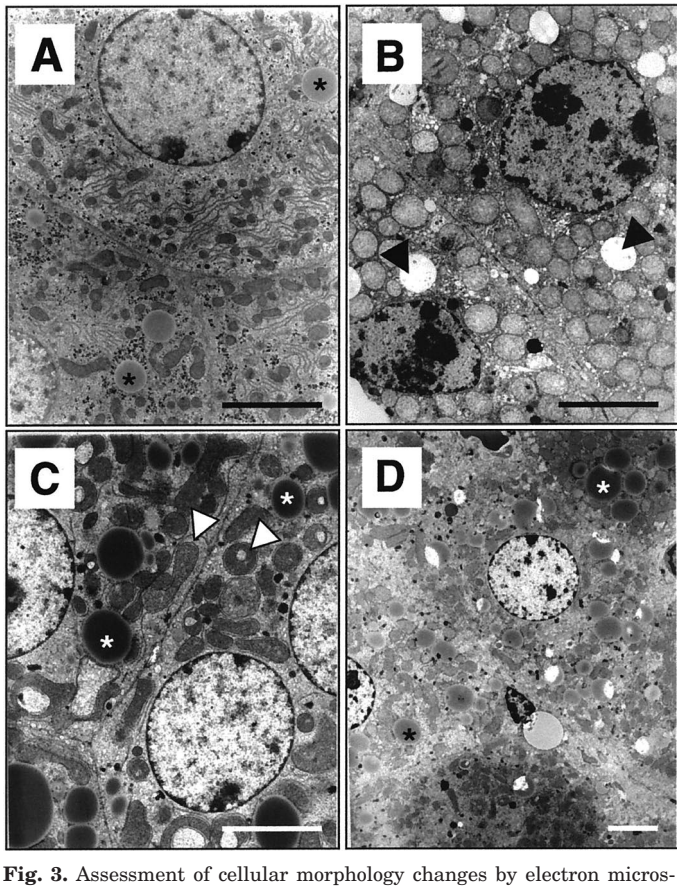

Fig. 3. Assessment of cellular morphology changes by electron microscopy. Liver sections were fixed in Karnovsky's fixative and stained with Reynold's lead citrate 6 h after dosing with APAP and AMAP 500 mg/kg i.p. A, control *bcl-2* (−/+) treated only with $ZnSO_4$ showing normal hepatocyte morphology. B, WT (−/−) animals 6 h after dosing with APAP showing lipid deposition (solid arrowheads), mitochondrial proliferation, and nuclear condensation. C–D, *bcl-2* (−/+) animals 6 h after dosing with APAP and AMAP, respectively. APAP treatment (C) shows association of the endoplasmic reticulum with the mitochondria and ring-shaped mitochondria (hollow arrowhead), whereas AMAP-treatment (D) shows almost normal morphology with the exception of electron dense aggregates, which are seen in all *bcl-2* (−/+) animals (*). All magnifications are ~12,000X except (D) at ~6,000×. Scale bar, 5 μm.

dismutase (data not presented), increases in peroxisomal catalase content were found in the heavy membrane (mitochondrial) fraction after APAP treatment in both *bcl-2* (−/−) and *bcl-2* (−/+) animals (Fig. 4C).

Immunoblot Detection of BCL-2. Expression of human *bcl-2* transgene was confirmed by immunoblotting mouse liver tissue homogenates with commercially available antisera directed to the N-terminal region of BCL-2 (N19; *Materials and Methods*), which recognizes both human and endogenous mouse BCL-2. The data demonstrated clearly an overexpression of the human *bcl-2* transgene in transgenic animals, whereas little or no endogenous murine BCL-2 was detected in WT mice (Fig. 5A, top). Immunoblotting also revealed apparent decreases in BCL-2 protein content in APAP- but not AMAP-treated transgenic mice relative to GAPDH loading controls (Fig. 5A, compare top and bottom blots). These slight decreases in BCL-2 protein seemed to correlate with an increased breakdown of mouse hepatic albumin in APAP-treated groups (Fig. 5A, compare top and middle blots) and could not be attributed to general sample proteolysis as the GAPDH loading standards remained unaffected (Fig. 5A, bottom blot).

Caspase Activation. BCL-2 degradation is generally associated with a proapoptotic state and increased activity of the effector caspase, caspase-3. To further examine the possibility of BCL-2 cleavage to its proapoptotic form by caspase-3, the activation of caspase-3-like enzymes in liver tissue homogenates was evaluated. Only modest increases in Ac-DEVD-amc cleavage were observed after either APAP- or AMAP-treatment of *bcl-2* (−/+) transgenic or WT mice (Fig. 5B). For example, at 6 h after treatment, AMAP-treated transgenic mice had the highest change in caspase-3-like activity (1.28-fold increase versus control, $p \leq 0.05$), whereas at 24 h after treatment, APAP-treated transgenic mice were

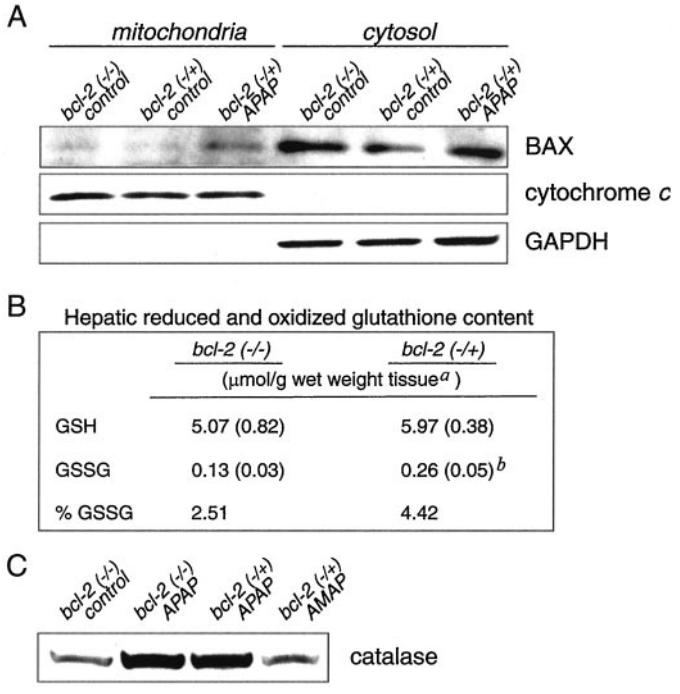

B

Hepatic reduced and oxidized glutathione content

	bcl-2 (-/-)	bcl-2 (-/+)
	(μmol/g wet weight tissue[a])	
GSH	5.07 (0.82)	5.97 (0.38)
GSSG	0.13 (0.03)	0.26 (0.05)[b]
% GSSG	2.51	4.42

Fig. 4. Biochemical characterizations of control, APAP-treated *bcl-2* (−/+), and WT (−/−) transgenic animals. A, subcellular BAX content from mitochondrial and cytosolic fractions prepared from *bcl-2* (−/−) and *bcl-2* (−/+) animals 2 h after treatment with vehicle only (saline/control) or APAP (500 mg/kg, i.p.) as described under *Materials and Methods*. APAP-specific BAX translocation to the mitochondrial fraction was observed in BCL-2 overexpressing animals (top blot). Cytochrome *c* and GAPDH remained in the mitochondria and cytosol, respectively, in all treatment groups (lower 2 blots). B, hepatic GSH and GSSG contents of *bcl-2* (−/−) and *bcl-2* (−/+) mice induced with $ZnSO_4$ in the drinking water for 5 to 7 days and dosed with saline vehicle only as described under *Materials and Methods*. a, total GSH or GSSG content reported as mean ± S.E. (n = 4); b, significant increase ($p < 0.05$) in GSSG in *bcl-2* (−/+) transgenic animals. C, APAP-specific elevations of hepatic catalase content in "heavy membrane" (mitochondria + peroxisomes) fractions of *bcl-2* (−/−) and *bcl-2* (−/+) animals isolated 6 h after vehicle or drug treatment.

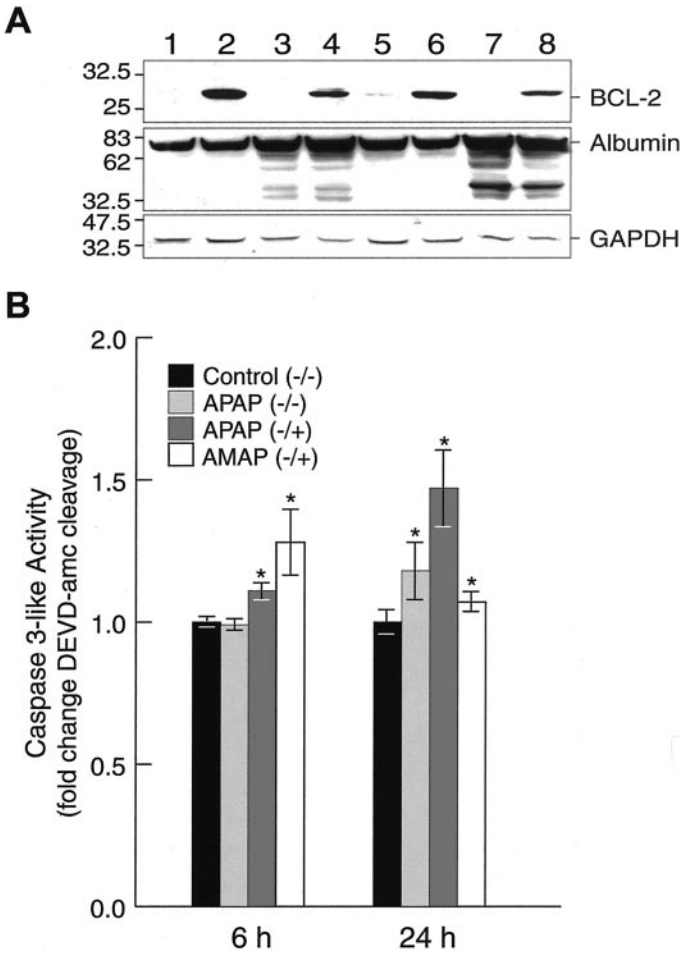

Fig. 5. BCL-2 transgene overexpression and caspase activities in control and APAP-dosed WT (−/−) and *bcl-2* (−/+) animals. A, confirmation by immunoblot analysis of liver BCL-2 content in tissue homogenates from control, APAP or AMAP (500 mg/kg, i.p.) treatments prepared as described under *Materials and Methods.* The blot was probed with antisera to BCL-2 (N19) (Santa Cruz), GAPDH, and albumin (ICN) using standard procedures. Molecular weight markers (kilodaltons) are indicated to the left of the panel. Samples were taken at 6 h (lanes 1–4) and 24 h (lanes 5–8) after treatment. Endogenous murine BCL-2 was not detected in saline-injected WT animals (lanes 1 and 5) or APAP-treated WT animals (lanes 3 and 7) using BCL-2 (N19) antiserum. High levels of BCL-2 expression were confirmed in *bcl-2* (−/+) animals treated with $ZnSO_4$ and dosed with AMAP (lanes 2 and 6) or APAP (lanes 4 and 8). Degradation of albumin was observed predominantly in the APAP-treated animals. Equal loading of samples was demonstrated by GAPDH content after membrane stripping, blocking and reprobing. B, the activation of caspase-3-like enzymes was evaluated as described under *Materials and Methods*. Activity is represented as fold change in Ac-DEVD-amc cleavage versus untreated animals after 60 min of incubation in caspase assay buffer. Error bars represent S.E. of mean expressed as a percentage of absolute activity and range from 1.1 to 6.2% of total activity. n = 3 to 6 animals for each treatment group. *$p < 0.05$ (compared with control values).

highest with a 1.47-fold increase in activity versus control ($p \leq 0.05$). These changes are in agreement with our previous studies, indicating only slight caspase-3-like activation after APAP-treatment in vitro and in vivo (Pierce et al., submitted). Although statistically significant the biological relevance of low-level Ac-DEVD-amc cleavage activity in APAP- and AMAP-treated mice observed in these studies is unclear.

Complex III Activities. To evaluate overall mitochondrial respiratory chain activity, ubiquinol:ferricytochrome *c* oxidoreductase (complex III) activity was determined in control and treatment groups. At 6 h and before overt liver damage, all three treatment groups demonstrated a statistically significant decrease in complex III activity compared with control levels (Fig. 6). The extent of inhibition correlated well with eventual liver damage as APAP-treated transgenic mice were most adversely affected (with the exception of AMAP-treatment; see next paragraph). The same trend was also seen in APAP-treated transgenic animals at 24 h when liver damage was well advanced but the absolute level of complex III inhibition was less. This may be a consequence of the differential centrifugation procedures used to isolate mitochondria from damaged tissue with the selection of intact, and relatively functional, organelles.

Compared with APAP-treated animals, however, AMAP-treated transgenic complex III activities had returned to control levels after 24 h in agreement with histopathological observations (Fig. 2). This provides further support for a transient complex III loss and subsequent recovery of mitochondrial function by this nonhepatotoxic isomer (Fig. 6). Observed changes in complex III activities at 24 h correlated well with plasma AST ($r^2 = 0.89$) and ALT ($r^2 = 0.87$) levels at the same time point, supporting the conclusion that mitochondrial function, and especially complex III activity, is an indicator of APAP-induced hepatotoxicity.

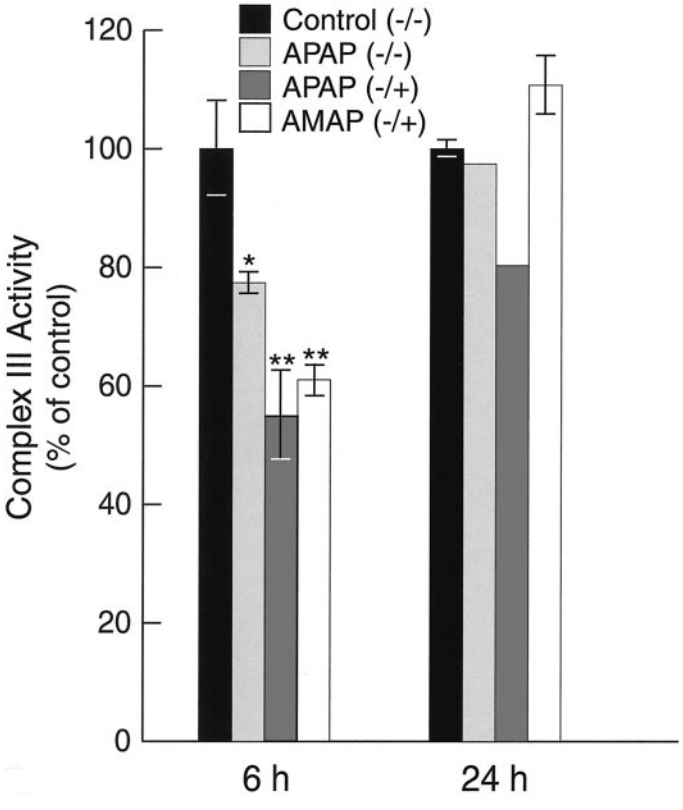

Fig. 6. Complex III activity. Complex III (ubiquinol:ferricytochrome *c* oxidoreductase) activities for each treatment group (APAP or AMAP, 500 mg/kg, i.p.) was determined as described under *Materials and Methods*. Values are reported as percentage of mean control rate (micromoles of cytochrome *c* reduced per minute per milligram of mitochondrial protein). Errors, expressed as percentage of S.E., ranged from 1.4 to 7% for control groups and 3.5 to 10.5% for treatment groups. $n = 3$ to 6 for all treatment groups except APAP (−/+) 24 h and APAP (−/−) 24 h for which $n = 2$. $^*p = 0.05$, $^{**}p < 0.05$ (compared with control values).

Discussion

The cell death and liver injury produced by APAP has been studied extensively for more than 20 years. Necrosis has usually been associated with APAP-induced hepatotoxicity; more recently, a role for apoptosis has been proposed but not supported by extensive data (Ray et al., 1996; Lawson et al., 1999). For example, studies have concluded that APAP-associated hepatotoxicity is a mixed necrotic and apoptotic event, with approximately 40% of cells undergoing apoptosis based on oligosomal DNA laddering, whereas 60% undergo necrosis as determined by plasma transaminase elevations (Ray et al., 1996). The data presented here suggest an early role for BAX in APAP-induced liver injury, indicating that necrotic cell death in these circumstances may be initiated at the mitochondrion in a proapoptotic manner. Nonetheless, the precise relationship between APAP-mediated protein modifications, mitochondrial BAX content, and cell death has yet to be fully determined.

Mitochondria play an important role in APAP-mediated cell death. This has been deduced from many studies that indicate preferential mitochondrial glutathione depletion, calcium deregulation (Tirmenstein and Nelson, 1989, 1991), and selective protein modifications within the mitochondrion (Qiu et al., 1998a,b) after APAP—but not AMAP—treatment. Consistent with general mitochondrial dysfunction, both decreased oxygen utilization and ATP levels have been associated with APAP overdosing (Tirmenstein and Nelson, 1990; Burcham and Harman, 1991). In a related observation, it has been proposed previously that ATP levels are critical in determining the path to cell death (i.e., apoptosis versus necrosis) (Leist et al., 1997).

Most studies have used protective agents to elucidate the mechanism by which APAP elicits its toxicity (e.g., antioxidants, calcium chelators). Our studies have focused on the events downstream of APAP-protein adduction and examined the cellular responses to such modifications that ultimately lead to cell death. BAX has been shown to regulate the release of mitochondrial cytochrome *c* via components of the permeability transition pore (Shimizu et al., 1999). Consequently, APAP- and AMAP-mediated cell death and liver injury may be attributable, at least in part, to this mechanism. Other contributing factors seem to be required, however, because mitochondrial BAX localization does not always correlate with cytochrome *c* loss into the cytosol (Figs. 1 and 4A; Putcha et al., 1999). In this regard, it should be noted that BAX-dependent mitochondrial cytochrome *c* release is insufficient to account for the capacity to undergo apoptosis in a trophic factor withdrawal model of sympathetic neuron cell death (Deshmukh and Johnson, 1998). An alternative explanation for the absence of cytochrome *c* in the cytosol, despite mitochondrial BAX localization, can be found with a recent report, which indicates that the absolute levels

of intracellular BAX may determine the extent and even reversibility of mitochondrial cytochrome *c* release (Pastorino et al., 1999). Finally, BAX-induced apoptosis requires a functional F_0F_1-ATPase proton pump in mammalian cells (Matsuyama et al., 1998), which may explain recent findings indicating that F_0F_1-ATPase inhibition protects against APAP-mediated damage (Banerjee et al., 1998).

It has also been recognized that BCL-2 itself, as well as other members, such as BCL-X_L (the BCL-2 functional homolog expressed in hepatocytes; Tzung et al., 1997), heterodimerize with BAX (e.g., Yin et al., 1994). BCL-2 dimerization with BAX is thought to mediate its antiapoptotic action (Yin et al., 1994; Rosse et al., 1998). Recognizing the function of BAX translocation as an initiating mitochondrial event in many apoptotic systems (Wei et al., 2001), and the potential for regulatory control by BCL-2, we have attempted to determine whether BCL-2 overexpression may protect against APAP-induced hepatotoxicity as reported for other stimuli (Rosse et al., 1998; Putcha et al., 1999). In this manner, perturbing the balance between BAX and BCL-2 in favor of BCL-2, should be hepatoprotective.

The liver damage we have observed in APAP-treated *bcl-2* (−/+) transgenic animals was considerably greater than that found with WT animals, contrary to our expectations (Fig. 2, Table 1). Moreover, we were able to detect APAP-specific localization of BAX to mitochondria in *bcl-2* (−/+) animals (Fig. 4A). However, these levels seemed to be considerably lower than those of comparably treated nontransgenic mice as determined by immunoblot sensitivity. The only measurable difference we have observed between control BCL-2–overexpressing and WT animals is an elevation of hepatic oxidized glutathione (GSSG) in *bcl-2* (−/+) animals (Fig. 4B). Although an antioxidant function has been attributed to BCL-2, our findings are in agreement with a previous report proposing a prooxidant capacity for BCL-2 (Steinman, 1995). In addition, it has also been observed that BCL-2 overexpression fails to prevent the action of classical inducers of permeability transition in isolated mouse liver mitochondria (Yang et al., 2000). Moreover, our caspase-3-like activities (Ac-DEVD-amc cleavage) were much lower than that observed with most other apoptosis models (Fig. 5B). This low-level caspase activation was expected based on previous reports of no caspase activation (Lawson et al., 1999) and our observations of low caspase activation in APAP- and AMAP-treated mice (Pierce et al., submitted). These observations are consistent with a proapoptotic initiation of liver damage during APAP overdose and subsequent advance to death via necrosis.

Disruption of oxidative phosphorylation, specifically at complex I and complex II, after direct exposure to NAPQI, the APAP reactive intermediate, has been previously reported (Burcham and Harman, 1991) but an inhibition of complex III in vivo has not been observed. However, in vitro studies have demonstrated decreased complex III activity after NAPQI exposure to inverted membrane particles (Ramsay et al., 1989). From the studies presented here we conclude that alterations to complex III activities can be a sensitive and early marker of the eventual extent of liver damage.

The generation of a proapoptotic BCL-2 cleavage fragment by caspase-3 or other proteolytic cleavage activity may offer an explanation for the enhanced APAP-induced hepatotoxicity we have observed (Cheng et al., 1997; Kirsch et al., 1999). Although our studies suggest that BCL-2 protein levels were decreased 24 h after APAP treatments, we have not detected BCL-2 fragments consistent with cleavage by caspase-3 to the proapoptotic form (Fig. 5A). Our data (i.e., low caspase activation and no evidence for a specific cleavage product) suggest that BCL-2 disappearance in animals treated with APAP for 24 h may be attributable to another cellular proteolytic activity (e.g., proteasome; Breitschopf et al., 2000; Pierce et al., submitted). Further experiments will be required to determine the mechanism of BCL-2 loss in APAP-treated animals. An alternative explanation for enhanced APAP-induced hepatotoxicity in BCL-2–overexpressing animals is the observation that APAP transiently inhibits proteasomal activity (Qiu et al., 1998b; Pierce et al. submitted). Finally, our data suggest the possibility that BCL-2 exacerbation of liver injury by APAP does not occur by a mitochondrially mediated mechanism for two reasons. BAX translocation in APAP-treated *bcl-2* (−/+) is not associated with cytochrome *c* release into the cytosol and peroxisomal catalase content was induced with APAP treatment adding to a basal, but apparently nonpathological, oxidative stress in untreated *bcl-2* (−/+) animals. Further studies will be required to determine the role of other organelles, and especially the ER, in this form of liver injury.

In conclusion, our studies indicate that the overexpression of human BCL-2 in C57/B6C3H mice significantly enhances APAP-induced hepatotoxicity. Biochemical and morphological evidence also confirms a key role for mitochondria in the progression of this damage. These novel findings allow for new avenues to approach and define the mechanism of APAP-mediated hepatotoxicity.

Acknowledgments

We thank Dr. Chris Franklin for his helpful conversations and his assistance with the caspase assay.

References

Adamson GM and Harman AW (1993) Oxidative stress in cultured hepatocytes exposed to acetaminophen. *Biochem Pharmacol* **45:**2289–2294.

Banerjee A, Linscheer WG, Chiji H, Murthy UK, Cho C, Nandi J, and Chan SH (1998) Induction of an ATPase inhibitor protein by propylthiouracil and protection against paracetamol (acetaminophen) hepatotoxicity in the rat. *Br J Pharmacol* **124:**1041–1047.

Breitschopf K, Haendeler J, Malchow P, Zeiher AM, and Dimmeler S (2000) Post-translational modification of Bcl-2 facilitates its proteasome-dependent degradation: molecular characterization of the involved signaling pathway. *Mol Cell Biol* **20:**1886–1896.

Burcham PC and Harman AW (1991) Acetaminophen toxicity results in site-specific mitochondrial damage in isolated mouse hepatocytes. *J Biol Chem* **266:**5049–5054.

Cai J and Jones DP (1998) Superoxide in apoptosis. Mitochondrial generation triggered by cytochrome *c* loss. *J Biol Chem* **273:**11401–11404.

Cheng EH, Kirsch DG, Clem RJ, Ravi R, Kastan MB, Bedi A, Ueno K, and Hardwick JM (1997) Conversion of Bcl-2 to a Bax-like death effector by caspases. *Science (Wash DC)* **278:**1966–1968.

Deshmukh M and Johnson EM (1998) Evidence of a novel event during neuronal death: development of competence-to-die in response to cytoplasmic cytochrome c. *Neuron* **21:**695–705.

Dietze EC, Schafer A, Omichinski JG, and Nelson SD (1997) Inactivation of glyceraldehyde-3-phosphate dehydrogenase by a reactive metabolite of acetaminophen and mass spectral characterization of an arylated active site peptide. *Chem Res Toxicol* **10:**1097–1103.

Dunn WA (1990) Studies on the mechanisms of autophagy: formation of the autophagic vacuole. *J Cell Biol* **110:**1923–1933.

Franklin CC, Srikanth S, and Kraft AS (1998) Conditional expression of mitogen-activated protein kinase phosphatase-1, MKP-1, is cytoprotective against UV-induced apoptosis. *Proc Natl Acad Sci USA* **95:**3014–3019.

Ghadially FN (1997) Mitochondria, in *Ultrastructural Pathology of the Cell and Matrix,* 4th ed, vol 1, pp 195–342, Butterworth-Heinemann, Boston.

Gudz TI, Tserng KY, and Hoppel CL (1997) Direct inhibition of mitochondrial respiratory chain complex III by cell-permeable ceramide. *J Biol Chem* **272:**24154–24158.

Haldar S, Basu A, and Croce CM (1998) Serine-70 is one of the critical sites for drug-induced Bcl2 phosphorylation in cancer cells. *Cancer Res* **58:**1609–1615.
Hockenbery DM, Oltvai ZN, Yin XM, Milliman CL, and Korsmeyer SJ (1993) Bcl-2 functions in an antioxidant pathway to prevent apoptosis. *Cell* **75:**241–251.
Kirsch DG, Doseff A, Chau BN, Lim DS, de Souza-Pinto NC, Hansford R, Kastan MB, Lazebnik YA, and Hardwick JM (1999) Caspase-3-dependent cleavage of Bcl-2 promotes release of cytochrome c. *J Biol Chem* **274:**21155–21161.
Lawson JA, Fisher MA, Simmons CA, Farhood A, and Jaeschke H (1999) Inhibition of Fas receptor (CD95)-induced hepatic caspase activation and apoptosis by acetaminophen in mice. *Toxicol Appl Pharmacol* **156:**179–186.
Leist M, Single B, Castoldi AF, Kuhnle S, and Nicotera P (1997) Intracellular adenosine triphosphate (ATP) concentration: a switch in the decision between apoptosis and necrosis. *J Exp Med* **185:**1481–1486.
Luderer U, Kavanagh TJ, White CC, and Faustman EM (2001) Gonadatropin regulation of glutathione synthesis in the rat ovary. *Reprod Toxicol.* In press.
Matsuyama S, Xu Q, Velours J, and Reed JC (1998) The Mitochondrial F_0F_1-ATPase proton pump is required for function of the proapoptotic protein Bax in yeast and mammalian cells. *Mol Cell* **1:**327–336.
Pastorino JG, Tafani M, Rothman RJ, Marcinkeviciute A, Hoek JB, Farber JL, and Marcineviciute A (1999) Functional consequences of the sustained or transient activation by Bax of the mitochondrial permeability transition pore. *J Biol Chem* **274:**31734–31739.
Pumford NR and Halmes NC (1997) Protein targets of xenobiotic reactive intermediates. *Annu Rev Pharmacol Toxicol* **37:**91–117.
Putcha GV, Deshmukh M, and Johnson EM Jr (1999) BAX translocation is a critical event in neuronal apoptosis: regulation by neuroprotectants, BCL-2, and caspases. *J Neurosci* **19:**7476–7485.
Qiu Y, Benet LZ, and Burlingame AL (1998a) Identification of mouse liver protein targets for reactive metabolites of nonhepatotoxic acetaminophen regioisomer, 3′-hydroxyacetanilide: a comparison of covalent binding spectrum with acetaminophen, in *Proceedings of the 46th ASMS Conference on Mass Spectrometry*; 1998 May 30–Jun 4; Orlando, Florida. Abstract 1136, American Society for Mass Spectrometry, Santa Fe, NM.
Qiu Y, Benet LZ, and Burlingame AL (1998b) Identification of the hepatic protein targets of reactive metabolites of acetaminophen in vivo in mice using two-dimensional gel electrophoresis and mass spectrometry. *J Biol Chem* **273:**17940–17953.
Ramsay RR, Rashed MS, and Nelson SD (1989) In vitro effects of acetaminophen metabolites and analogs on the respiration of mouse liver mitochondria. *Arch Biochem Biophys* **273:**449–457.
Ray SD, Mumaw VR, Raje RR, and Fariss MW (1996) Protection of acetaminophen-induced hepatocellular apoptosis and necrosis by cholesteryl hemisuccinate pretreatment. *J Pharmacol Exp Ther* **279:**1470–1483.
Redlich CA, West AB, Fleming L, True LD, Cullen MR, and Riely CA (1990) Clinical and pathological characteristics of hepatotoxicity associated with occupational exposure to dimethylformamide. *Gastroenterology* **99:**748–757.
Rosse T, Olivier R, Monney L, Rager M, Conus S, Fellay I, Jansen B, and Borner C (1998) Bcl-2 prolongs cell survival after Bax-induced release of cytochrome c. *Nature (Lond)* **391:**496–499.
Shimizu S, Narita M, and Tsujimoto Y (1999) Bcl-2 family proteins regulate the release of apoptogenic cytochrome c by the mitochondrial channel VDAC. *Nature (Lond)* **399:**483–487.
Steinman HM (1995) The Bcl-2 oncoprotein functions as a prooxidant. *J Biol Chem* **270:**3487–3490.
Tirmenstein MA and Nelson SD (1989) Subcellular binding and effects on calcium homeostasis produced by acetaminophen and a nonhepatotoxic regioisomer, 3′-hydroxyacetanilide, in mouse liver. *J Biol Chem* **264:**9814–9819.
Tirmenstein MA and Nelson SD (1990) Acetaminophen-induced oxidation of protein thiols. Contribution of impaired thiol-metabolizing enzymes and the breakdown of adenine nucleotides. *J Biol Chem* **265:**3059–3065.
Tirmenstein MA and Nelson SD (1991) Hepatotoxicity after 3′-hydroxyacetanilide administration to buthionine sulfoximine pretreated mice. *Chem Res Toxicol* **4:**214–217.
Tonge RP, Kelly EJ, Bruschi SA, Kalhorn T, Eaton DL, Nebert DW, and Nelson SD (1998) Role of CYP1A2 in the hepatotoxicity of acetaminophen: investigations using Cyp1a2 null mice. *Toxicol Appl Pharmacol* **153:**102–108.
Tzung SP, Fausto N, and Hockenbery DM (1997) Expression of Bcl-2 family during liver regeneration and identification of Bcl-x as a delayed early response gene. *Am J Pathol* **150:**1985–1995.
Wei MC, Zong W-X, Cheng EH-Y, Lindsten T, Panoutsakopoulou V, Ross AJ, Roth KA, MacGregor GR, Thompson CB, and Korsmeyer SJ (2001). Proapoptotic BAX and BAK A requisite gateway to mitochondrial dysfunction and death. *Science (Wash DC)* **292:**727–730.
Yang JC, Kahn A, and Cortopassi G (2000) Bcl-2 does not inhibit the permeability transition pore in mouse liver mitochondria. *Toxicology* **151:**65–72.
Yin XM, Oltvai ZN, and Korsmeyer SJ (1994) BH1 and BH2 domains of Bcl-2 are required for inhibition of apoptosis and heterodimerization with Bax. *Nature (Lond)* **369:**321–323.

Address correspondence to: Sam A. Bruschi, Ph.D., Department of Medicinal Chemistry, Box 357610, University of Washington, Seattle WA 98195-7610. E-mail: sambru@u.washington.edu